MATERIALS CHEMISTRY FRONTIERS

RESEARCH ARTICLE

View Article Online
View Journal

Cite this: DOI: 10.1039/d5qm00730e

Post-polymerization modification and release of functional groups based on an NIR light-emitting organoboron π-conjugated polymer

Masashi Nakamura, [a] Masayuki Gon [ab] and Kazuo Tanaka *[ab]

Received 9th October 2025,
Accepted 3rd February 2026

DOI: 10.1039/d5qm00730e

rsc.li/frontiers-materials

We developed a near-infrared (NIR) light-emitting organoboron π-conjugated polymer that can be functionalized through post-polymerization modification with click chemistry. The perpendicularly protruding substituents at the boron center are reactive and almost electronically independent from the polymer main chain. These properties allow the quantitative chemical modification of functional groups as side-chains even after polymerization, without any influence on the main-chain properties. In particular, to the best of our knowledge, we first demonstrate that the boron-fused azobenzene complex can release the introduced functional units at the boron center upon treatment with reactive agents, such as nucleophilic bases and photo-radical initiators. We observed that the release of pyrene side-chains can be monitored by the disappearance and appearance of the NIR and blue emissions, respectively, even for water-dispersible polymer nanoparticles. This study provides a novel design strategy for stimuli-responsive theranostic systems based on NIR-fluorescent π-conjugated polymers.

Introduction

Post-polymerization modification (PPM) is a powerful method for combining multiple functions and improving the performance of polymeric materials. A single precursor can be easily transformed into diversely functionalized polymers, enabling the fine-tuning of properties with less demanding synthetic and purification steps compared to the traditional approach of polymerizing functionalized monomers.[1–5] In addition, PPM allows the introduction of functional groups that are incompatible under the polymerization conditions. Click chemistry, represented by copper-catalyzed alkyne–azide cycloaddition (CuAAC), is one of the most prevailing synthetic approaches for PPM because of its excellent reliability toward various substances with high yield and superior selectivity.[6–8] Furthermore, selective and orthogonal PPM is achieved by combining different types of reactions, such as thiol–ene,[9] thiol–yne,[10] nitrile oxide–olefin cycloaddition,[11] pentafluorophenyl substitution,[12] and sulfur(VI) fluoride exchange.[13] These synthetic approaches have provided multifunctional platforms, especially for drug delivery, such as polymer–drug conjugates with targeting agents[14–17] and theranostic materials that combine diagnostic and therapeutic units in one polymer system.[18–21] Such a "one-for-all" approach shows promise as a strategy for achieving a simplified fabrication process and good reproducibility compared with the conventional "all-in-one" approach, in which different functional materials are integrated into nanoparticles (NPs) through covalent or non-covalent interactions.[22] In general, the "all-in-one" approach is easy to implement and has broad substrate applicability. However, it is difficult to avoid competing effects among the included components, which may reduce reproducibility. In contrast, the "one-for-all" approach provides better reproducibility owing to the use of multifunctional platforms based on the sophisticated molecular design. Therefore, there is a need to design new multifunctional platforms to meet various demands.

Near-infrared (NIR, >700 nm) fluorescence (FL) imaging is a powerful diagnostic technique owing to its deep-tissue penetration ability and high spatial and temporal resolutions.[23–25] To date, theranostic agents that combine NIR light-emitting small molecules for diagnosis with polymer–drug conjugates for therapy have been reported.[26–28] In addition to π-conjugated fluorophores based on small molecules that have been actively studied, fluorescent π-conjugated polymers are beneficial in terms of their high brightness, attributed to the superior light-absorption property derived from their extended π-conjugated system.[29] However, very few theranostic agents in which drugs or some therapeutic units are conjugated to NIR-fluorescent π-conjugated polymers have been reported. This is likely due to a lack of monomers that satisfy both the NIR FL and PPM requirements.

[a] Department of Polymer Chemistry, Graduate School of Engineering, Kyoto University Katsura, Nishikyo-ku, Kyoto 615-8510, Japan. E-mail: tanaka@poly.synchem.kyoto-u.ac.jp
[b] Department of Technology and Ecology, Graduate School of Global Environmental Studies, Kyoto University Katsura, Nishikyo-ku, Kyoto 615-8510, Japan

Our group has recently reported a novel class of donor–acceptor (D–A)-type π-conjugated polymers capable of highly efficient NIR fluorescence.[30,31] The key building block is a boron-fused azobenzene complex (BAz) created by a tridentate azobenzene ligand and boron.[32] The intrinsic strong electron-accepting ability of BAz plays a critical role in achieving the narrow energy gap between the frontier molecular orbitals, thereby enabling NIR FL in the resulting polymer. In addition, the simple modification of BAz can enhance its electron-accepting character[33] and extend the fluorescent property of the resulting polymer into the second NIR (NIR-II, >1000 nm) region.[34] Furthermore, the π-conjugated system of the main chain and the perpendicularly protruded substituents at the boron center are almost electronically independent. Based on this structural feature, additional functions could be introduced *via* modification at the boron center without compromising the NIR FL property of the polymer main-chain.[35–37]

Meanwhile, stimuli-responsive properties can be imparted by incorporating reactive parts to the resulting polymers, leading to on-demand drug release and elaborate sensing systems for some *in vivo* reactants. Boron is one of the potential elements capable of serving as the responsive unit because of its unique reactivity with nucleophiles, and a series of sensing materials have been established based on fluorescent organoboron compounds with π-conjugated systems.[38–42] In addition, materials including boron are beneficial as carriers in boron neutron capture therapy (BNCT).[43–45] If the release of the functional units introduced at the boron center, triggered by external stimuli, is coupled with changes in the FL property, quantitative information on drug distribution and concentration could be obtained, as well as real-time monitoring of treatment progress.

The implementation of molecular functionalization at the boron center using click chemistry has been reported. Workentin, Gilroy and coworkers performed the CuAAc reaction with dialkynylborane complexes of the bidentate formazanate ligand.[46] They achieved the asymmetric functionalization of the boron-stereogenic compounds by the enantioselective CuAAc reaction.[47] Therefore, the system is still epoch-making in terms of the development of π-conjugated polymers with both PPM capability and NIR FL. Here, we demonstrate PPM of the substituents at the boron center in an NIR light-emitting π-conjugated polymer composed of an azide group-substituted BAz derivative. When pyrene was loaded onto the boron center *via* the CuAAC reaction, energy transfer from the pyrene to the polymer backbone occurred, resulting in the observation of only NIR FL from the polymer backbone. Through treatments with nucleophilic bases or radicals, the boron atom was eliminated from the conjugated system, and a concomitant decrease in the NIR and an increase in the blue FL from the pyrene were observed. As a result, the release of the boron unit can be monitored through both NIR emission quenching and blue emission enhancement. Furthermore, these releasing behaviors were able to be realized in the water-dispersible NP using a surfactant triggered by ultraviolet (UV) light irradiation. By leveraging the structural features and reactivity of boron, new controlled-release systems can be established.

Results and discussion

Synthesis and characterization

The synthetic procedure is shown in Fig. 1a. First, the BAz derivative with an azide group at the boron center (**N_3-Br**) was obtained by the condensation reaction between the azobenzene tridentate ligand (**OH-Br**)[36] and potassium 4-(azidomethyl)phenyltrifluoroborate. This reaction was conducted with diisopropylethylamine (DIEA) as a base and trimethylsilyl trifluoromethanesulfonate (TMSOTf) as a Lewis acid in acetonitrile (MeCN) at room temperature, affording a 28% isolated yield. Next, the Migita–Kosugi–Stille cross-coupling polymerization was carried out with 5,5′-bis(trimethylstannyl)-3,3′-dodecyl-2,2′-bithiophene (**BT**)[48,49] under a catalytic condition using $Pd_2(dba)_3$ (dba = dibenzylideneacetone) and 2-dicyclohexylphosphino-2′,4′,6′-triisopropylbiphenyl (XPhos). Reprecipitation with the obtained polymeric products from methanol afforded the D–A π-conjugated polymer (**P-N_3-BT**) in 70% isolated yield. The PPM of **P-N_3-BT** was conducted by the CuAAC reaction with 1-ethynylpyrene, copper(I) bromide (CuBr) as a catalyst and *N*,*N*,*N*′,*N*″,*N*″-pentamethyl-diethylenetriamine (PMDTA) as a base in tetrahydrofuran (THF). Unreacted 1-ethynylpyrene was completely removed *via* high-performance liquid chromatography (HPLC), and the pyrene-modified polymer (**P-py-BT**) was prepared in 31% isolated yield. Although the click reaction is known to proceed almost quantitatively, some losses occurred during the purification processes to obtain pure **P-py-BT**. The ^{1}H NMR spectrum of **P-py-BT** indicated that the CuAAc reaction proceeded quantitatively (Fig. 1b). Gel permeation chromatography (GPC) was conducted with polystyrene standards using chloroform ($CHCl_3$) as an eluent, and the chromatogram of **P-py-BT** after HPLC was almost identical to that of **P-N_3-BT**, suggesting that decomposition was negligible during the reaction (Table 1). The slight decrease in the calculated molecular weights in **P-py-BT** might be attributed to the alteration of the polymer hydrodynamic radius derived from the functionalized bulkier side-chains. All synthesized compounds showed good solubility in common organic solvents, such as THF, $CHCl_3$, and dichloromethane (CH_2Cl_2), and good stability in ambient atmosphere. The chemical structures were confirmed by ^{1}H, ^{13}C{^{1}H}, ^{11}B NMR spectroscopy, high-resolution mass spectrometry (HRMS), and elemental analyses (see the SI).

Optical properties

To evaluate the optical properties of the obtained polymers, we evaluated their UV-vis-NIR absorption spectra, FL spectra, and absolute FL quantum yields (Φ_{FL}) in THF solution. The longest wavelengths of absorption and FL maxima (λ_{abs} and λ_{FL}, respectively), as well as the emission efficiency, of **P-py-BT** were identical to those of **P-N_3-BT**, indicating that PPM hardly affected the optical properties of the polymer main-chains. (Fig. 2a, b and Table 2). In the absorption spectra of **P-py-BT**,

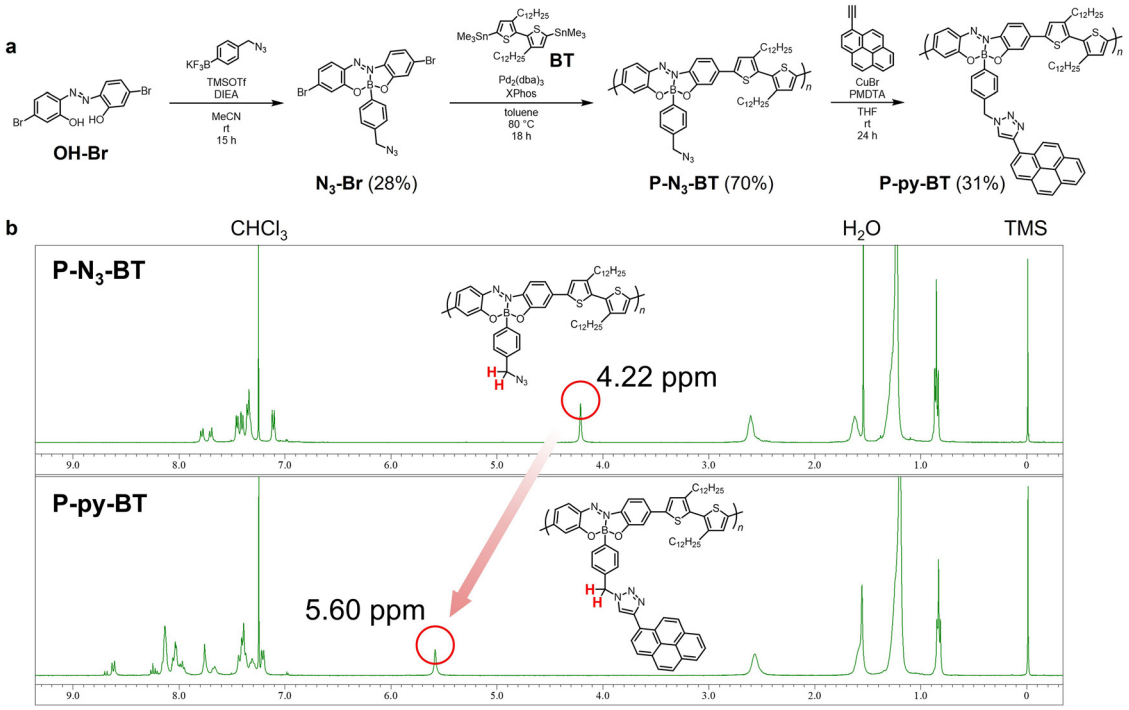

Fig. 1 (a) Synthetic scheme for **P-py-BT**. The regiorandom polymers are obtained, and only one representative structure is shown here. (b) ^{1}H NMR spectra in $CDCl_3$ (400 MHz), and chemical structures of **P-N$_3$-BT** and **P-py-BT**. Red circles indicate the signals of the methylene protons adjacent to the azido group for **P-N$_3$-BT** and the 1,2,3-triazole group for **P-py-BT**.

Table 1 Molecular weights and isolated yields of **P-N$_3$-BT** and **P-py-BT**

	M_n[a]	M_w[a]	M_w/M_n	n[b]	Yield/%
P-N$_3$-BT	15.1	38.3	2.54	17	70
P-py-BT	14.4	30.9	2.15	13	31

[a] Determined by gel permeation chromatography (GPC) with polystyrene standards. [b] Number-average degree of polymerization.

Table 2 Optical properties of **P-N$_3$-BT** and **P-py-BT** in THF (1.0×10^{-5} M per repeating unit)

	λ_{abs}/nm	λ_{ex}/nm (ε/cm^{-1} M^{-1})	λ_{FL}[a]/nm	Φ_{FL}[b]/%
P-N$_3$-BT	647	647 (81 860)	769	7.1
P-py-BT	647	647 (72 080)	769	7.2
	348	348 (42 140)	769, 407, 387	6.6[c]/—[de]

[a] Excited at λ_{ex}. λ_{ex}: excitation wavelength. [b] Absolute FL quantum yield, excited at λ_{ex}. [c] The Φ_{FL} value of emission from 660 to 950 nm. [d] The Φ_{FL} value of emission from 360 to 550 nm. [e] Not detected.

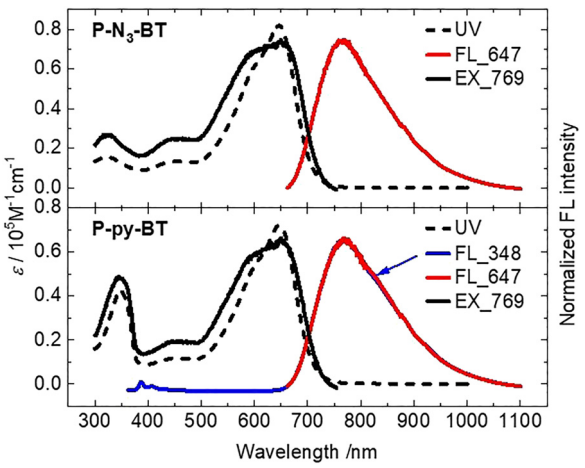

Fig. 2 UV-vis-NIR absorption, normalized FL, and normalized EX spectra of (top column) **P-N$_3$-BT** and (bottom column) **P-py-BT** in THF (1.0×10^{-5} M per repeating unit), excited at 348 and 647 nm for the FL spectra and monitored at 769 nm for the EX spectra.

an extra broadband peak at 348 nm derived from triazole-substituted pyrene was observed. Upon excitation of the pyrene moiety, the same NIR emission band was detected as that obtained upon excitation of the π-conjugated system of the polymer backbone. Although the blue emission of the pyrene was observable, it was too weak to estimate the emission efficiency. The excitation (EX) spectra of **P-py-BT** detected at the maximum FL wavelength were similar to the corresponding absorption spectra, including the broadband in the UV region, derived from pyrene. These results clearly indicate that energy transfer from the pyrene to the polymer backbone occurs.[37] From FL lifetime measurements (Fig. S1), **P-N$_3$-BT** and **P-py-BT** showed similar averaged FL lifetimes (τ_{av} = 0.27 ns for **P-N$_3$-BT** and τ_{av} = 0.28 ns for **P-py-BT**) upon excitation at longer absorption bands with a 504 nm laser diode while monitoring the NIR emission (λ_{FL} = 769 nm). On the other hand, **P-py-BT** exhibited a slightly longer average FL lifetime (τ_{av} = 0.31 ns) than **P-N$_3$-BT**

(τ_{av} = 0.27 ns) upon excitation at shorter absorption bands, including the absorption band of the pyrene unit, with a 375 nm laser diode while monitoring the NIR emission (λ_{FL} = 769 nm). Furthermore, when monitoring emission from the pyrene unit (λ_{FL} = 407 nm) in **P-py-BT**, the very short lifetime component ($\tau < 0.01$ ns) was dominant (95%). These results also indicate that energy transfer proceeds from the pyrene to the polymer backbone in **P-py-BT**.

Next, we conducted decomposition tests to assess stimuli-responsive behavior in terms of changes in the optical properties. Nucleophilic bases and radicals were selected as reactants that could attack the boron moiety. To ensure the reactivity of these reactants and the solubility of **P-py-BT**, purified THF without any undesirable radical species was used as a solvent.[50]

At first, the responsiveness was evaluated by treatment with 300 equivalents of nucleophilic bases toward the repeating unit of **P-py-BT**. Tetrabutylammonium hydroxide (TBAOH) was selected as the base because the hydrophobic cation has a high affinity for organic solvents and hydrophobic π-conjugated polymers. As shown in Fig. 3a, a gradual change in the solution color from blue to reddish purple was observed after adding TBAOH. In the UV-vis-NIR absorption spectra, λ_{abs} shifted from 647 nm to 568 nm with a large decrease in the molar extinction coefficient (ε) after 1 hour of incubation following base addition. In the FL spectra in Fig. 3b, the NIR FL completely disappears following base treatment, and intense blue FL appears instead. This is because the pyrene moiety is released, and subsequently, emission from the pyrene moiety is recovered. According to the GPC profiles, a broad peak derived from the fragmentated polymer products was observed after the base treatment, as well as a peak originating from the pristine polymer (Fig. S2). Thus, the decomposition likely started from the nucleophilic attack of the base to the boron or the azobenzene moieties, followed by the release of the boron moiety from the polymer main chain, accompanied by the partial decomposition of the polymer main chain.

Next, we investigated the responsiveness toward radicals. To generate radical species *in situ*, 100 equivalents of a photo-radical generator, 2,2-dimethoxy-2-phenylacetophenone (DMPA), toward the repeating unit of **P-py-BT** were added, and UV light at 365 nm was applied for 5 min with a transilluminator. Interestingly, the longest absorption band completely disappeared, and the solution turned colorless from light blue in **P-py-BT** with DMPA after the UV irradiation (Fig. 3c). In the GPC profile of the solution treated with the radical, the original high-molecular-weight peak disappeared and shifted to a lower-molecular-weight region. In addition, the NIR FL was annihilated, and intense blue emission appeared (Fig. 3d). In contrast, absorption and NIR FL spectra were maintained in the absence of DMPA even with UV light irradiation (Fig. 3c and d). These results suggest that the release of the introduced pyrene occurs simultaneously with the decomposition of the π-conjugated system in the polymer main-chain.

To gain further information on the pathways of the above-mentioned two reactions with the base and radical, we examined the decomposition products by HRMS using model compounds **BT-py-BT** and **BT-OH-BT** (Fig. 4). According to the data, the signal attributable to an aniline analogue, which results from the hydrolysis of the azobenzene moiety, was detected

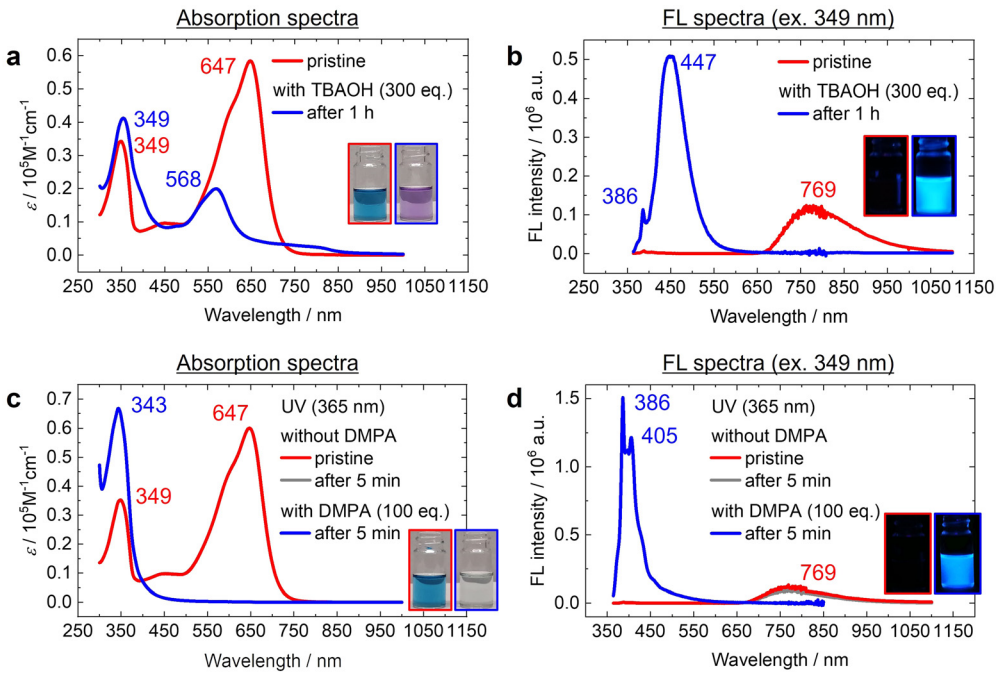

Fig. 3 (a) UV-vis-NIR absorption and (b) FL spectra of **P-py-BT** in THF (1.0×10^{-5} M per repeating unit) before and after base treatments, excited at 349 nm. (c) UV-vis-NIR absorption and (d) FL spectra of **P-py-BT** in THF (1.0×10^{-5} M per repeating unit) before and after UV irradiation under the condition with or without DMPA, excited at 349 nm. Red lines (pristine) and gray lines (after 5 min without DMPA) overlap.

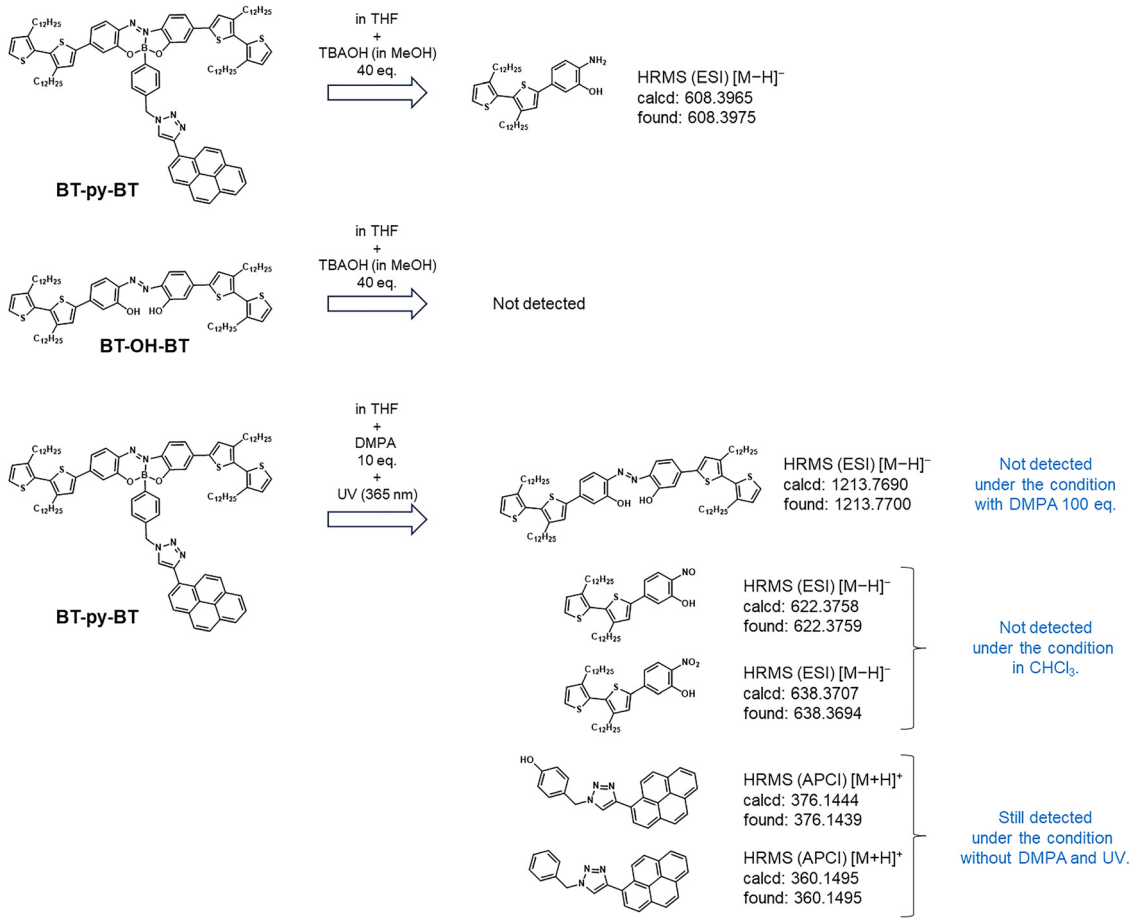

Fig. 4 Plausible decomposition mechanism. Molecular weights obtained from the HRMS spectra of the decomposition products.

from **BT-py-BT** but not from **BT-OH-BT** under the same conditions. Although there have been no reports on the hydrolysis of azo groups, to the best of our knowledge, it is proposed that the azo group could be hydrolyzed by activation through boron coordination. Considering the fact that the high molecular-weight polymers remained in the GPC profiles (Fig. S2), the release of the boron moiety might prevent the hydrolysis of the azo groups and the subsequent decomposition of the polymer main chain.

Next, we examined the reaction products after the introduction of the radical generator. After UV irradiation with the THF solution of **BT-py-BT** with DMPA (10 eq.), significant mass signals attributable to nitrosobenzene and nitrobenzene analogues were detected, which result from oxidation of the azobenzene moiety. These chemical species were not observed in the $CHCl_3$ solution, suggesting that the peroxides present in trace amounts in THF may be responsible for generating the oxidized products. In addition, **BT-OH-BT** was observed as one of the decomposition products with 10 eq. of DMPA, while it was not detected with a larger amount of DMPA (100 eq.). This implied that both the oxidation of the azo group and the desorption of the boron atom occur, and the latter might be the faster reaction. The decomposition products derived from the boron substituents, which could be formed by the reaction with oxygen radicals and peroxides, were also detected. However, it could be argued that these species derived from the boron moiety are merely fragments generated during the ionization in HRMS since the same species were found in the pure **BT-py-BT** solution subjected to neither DMPA addition nor UV irradiation.

Finally, the validity of the substance-release system triggered by UV irradiation was investigated in water. We fabricated a clear aqueous solution of an NP containing **P-py-BT** and DMPA (100 eq.) with the nanoprecipitation method, aided by the amphiphilic polymer DSPE-PEG(2000)-amine (Fig. 5a). The detailed preparation methods of the NPs are shown in the Electronic SI. The pristine NP exhibited NIR FL with Φ_{FL} of 3.1% even in water upon 349 nm excitation. After about 30 seconds of UV irradiation (365 nm) with a handy lamp, the solution turned colorless and simultaneously began to show blue FL (Movies S1 and S2). Finally, the reaction seemed to reach completion after 2 minutes of irradiation. We monitored the dispersion state with dynamic light scattering (DLS) and transmission electron microscopy (TEM) (Fig. S3). Accordingly, it was shown that the average hydrodynamic diameter of the pristine NPs was 50–60 nm with monodispersity, and the monodisperse nature was maintained after photoirradiation. The absorption and FL spectra before and after UV irradiation are shown in Fig. 5b and c, respectively. As observed for the

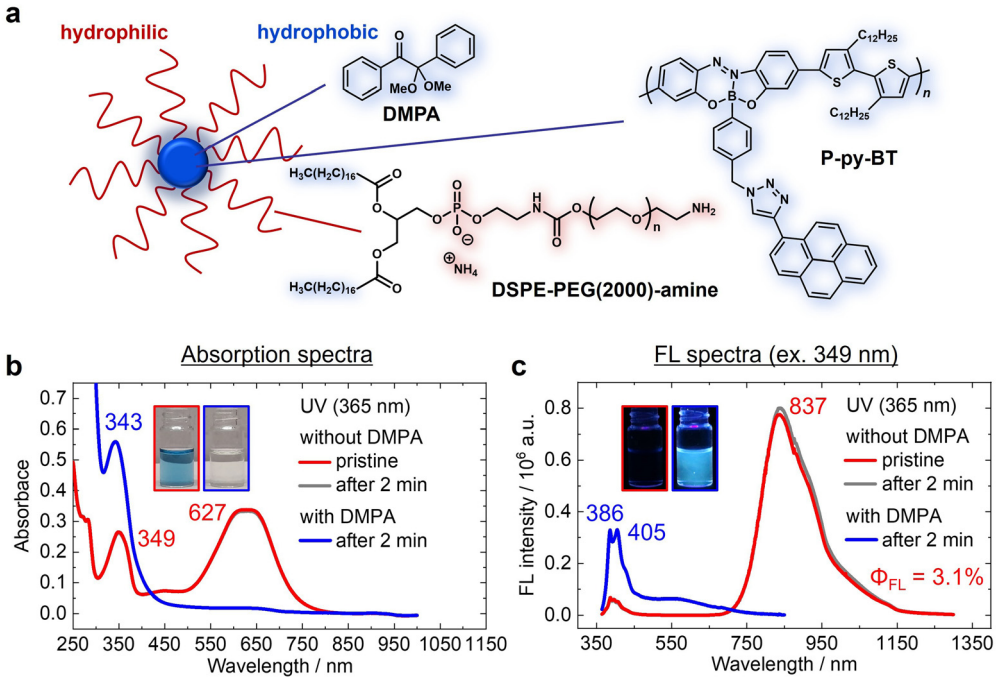

Fig. 5 (a) Schematic of the NP components. NPs are formed with hydrophobic and hydrophilic interactions and are able to be homogeneously dispersed in water. (b) UV-vis-NIR absorption spectra and (c) FL spectra of the NPs in water (1.0×10^{-5} M per repeating unit) before and after UV irradiation with or without DMPA, with excitation at 349 nm. Red lines (pristine) and gray lines (after 2 min without DMPA) overlap.

experiment in the THF solution, the longest absorption band around 630 nm and the NIR FL band completely disappeared, and a simultaneous enhancement of the blue FL band was observed. In addition, the spectral change was hardly detected for the NP without DMPA. Therefore, it was clarified that the NP can release the introduced functional units at the desired timing in water. In summary, it can be demonstrated that **P-py-BT** possesses a mechanism that allows a turn-on/-off behavior, reflecting a release of the functional units modified through PPM and the degradation at the boron part.

Conclusion

We developed a novel organoboron π-conjugated polymer that can be functionalized after polymerization. The azide groups at the boron center isolated from the π-conjugated system were able to be quantitatively modified by the CuAAC reaction even after polymerization, and the intrinsic NIR light-emitting property of the polymer main-chain was preserved. This method potentially allows us to introduce appropriate biological targeting agents and therapeutic substances. Focusing on the reactivity of the boron moiety, we discovered that the pyrene-introduced polymer (**P-py-BT**) exhibited release behavior, as evidenced by the FL response. Upon treatment with the base or the radical, a simultaneous decrease in the NIR FL and increase in the pyrene-derived FL were detected because of the elimination of the boron moiety and recovery of emission from the released pyrene moiety. The mechanistic study using HRMS and GPC suggested that the main decomposition route starts at the boron moiety; while the scission of the polymer main-chain can occur under basic conditions, it proceeds fully under radical conditions. Remarkably, the substance release in water triggered by UV irradiation and the associated change in the apparent and fluorescent color were achieved in the NP of **P-py-BT**. By using two-photon absorption techniques guided by NIR fluorescence, selective radical generation within deep tissue and the monitoring of the subsequent release of drugs by the decrease in the NIR emission can be expected. This research provides a positive proof-of-concept for multifunctional theranostic reagents that exhibit stimuli-responsive and NIR light-emitting properties, offering potential for real-time monitoring applications in biomedical and BNCT fields.

Conflicts of interest

There are no conflicts to declare.

Data availability

All experimental and characterization data and detailed experimental procedures are available in the published article and supplementary information (SI). Supplementary information: instrumentations, materials, synthetic procedures, characteristic data (^{1}H, ^{13}C{^{1}H}, ^{11}B NMR spectra, and HRMS), and experimental data (FL lifetime measurements, GPC chromatograms, and preparation methods and characterization of NPs). See DOI: https://doi.org/10.1039/d5qm00730e.

Acknowledgements

This work was partially supported by the National Research Foundation of Korea (NRF) grant funded by the Korea government (MSIT) (no. RS-2024-00406152), the Kansai Research Foundation for Technology Promotion (for M. G.), and the Japan Society for the Promotion of Science (JSPS) through a Grant-in-Aid for Scientific Research (B) (JP25K01818) (for M. G.) and (JP24K01570) (for K. T.).

References

1 K. A. Günay, P. Theato and H. Klok, Standing on the shoulders of Hermann Staudinger: post-polymerization modification from past to present, *J. Polym. Sci., Part A: Polym. Chem.*, 2013, **51**, 1–28.
2 T. J. Farmer, J. W. Comerford, A. Pellis and T. Robert, Post-polymerization modification of bio-based polymers: maximizing the high functionality of polymers derived from biomass, *Polym. Int.*, 2018, **67**, 775–789.
3 M. Rimmele, F. Glöcklhofer and M. Heeney, Post-polymerisation approaches for the rapid modification of conjugated polymer properties, *Mater. Horiz.*, 2022, **9**, 2678–2697.
4 A. Krusenbaum, S. Grätz, G. T. Tigineh, L. Borchardt and J. G. Kim, The mechanochemical synthesis of polymers, *Chem. Soc. Rev.*, 2022, **51**, 2873–2905.
5 J. Kockelmann, R. Zentel and L. Nuhn, Post-polymerization modifications to prepare biomedical nanocarriers with varying internal structures, their properties and impact on protein corona formation, *Macromol. Chem. Phys.*, 2023, **224**, 2300199.
6 M. Meldal and C. W. Tornøe, Cu-catalyzed azide−alkyne cycloaddition, *Chem. Rev.*, 2008, **108**, 2952–3015.
7 B. S. Sumerlin and A. P. Vogt, Macromolecular engineering through click chemistry and other efficient transformations, *Macromolecules*, 2010, **43**, 1–13.
8 B. Pektas, G. Sagdic, O. Daglar, S. Luleburgaz, U. S. Gunay, G. Hizal, U. Tunca and H. Durmaz, Ultrafast synthesis of dialkyne-functionalized polythioether and post-polymerization modification via click chemistry, *Polymer*, 2022, **253**, 124989.
9 L. M. Campos, K. L. Killops, R. Sakai, J. M. J. Paulusse, D. Damiron, E. Drockenmuller, B. W. Messmore and C. J. Hawker, Development of thermal and photochemical strategies for thiol−ene click polymer functionalization, *Macromolecules*, 2008, **41**, 7063–7070.
10 J. A. van Hensbergen, R. P. Burford and A. B. Lowe, ROMP (co)polymers with pendent alkyne side groups: post-polymerization modification employing thiol–yne and CuAAC coupling chemistries, *Polym. Chem.*, 2014, **5**, 5339–5349.
11 I. Singh, Z. Zarafshani, F. Heaney and J.-F. Lutz, Orthogonal modification of polymer chain-ends via sequential nitrile oxide–alkyne and azide–alkyne Huisgen cycloadditions, *Polym. Chem.*, 2011, **2**, 372–375.
12 N. ten Brummelhuis and M. Weck, Orthogonal multifunctionalization of random and alternating copolymers, *ACS Macro Lett.*, 2012, **1**, 1216–1218.
13 J. S. Oakdale, L. Kwisnek and V. V. Fokin, Selective and orthogonal post-polymerization modification using sulfur(VI) fluoride exchange (SuFEx) and copper-catalyzed azide–alkyne cycloaddition (CuAAC) reactions, *Macromolecules*, 2016, **49**, 4473–4479.
14 R. Pola, A. Braunová, R. Laga, M. Pechar and K. Ulbrich, Click chemistry as a powerful and chemoselective tool for the attachment of targeting ligands to polymer drug carriers, *Polym. Chem.*, 2014, **5**, 1340–1350.
15 M. Arslan, B. S. Bolu, R. Sanyal and A. Sanyal, A modular and orthogonally reactive platform for fabrication of polymer–drug conjugates for targeted delivery, *Polym. Chem.*, 2020, **11**, 7137–7146.
16 J. Xu, S. Lin, H. Hu, Q. Xing and J. Geng, Tumor-targeting polymer–drug conjugate for liver cancer treatment in vitro, *Polymers*, 2022, **14**, 4515.
17 Z. Liu, H. Zhang, J. Sun, M. Zheng, L. Cui, Y. Zhang, J. Cheng, Z. Tang and X. Chen, Organic-solvent-free ''lego-like'' modular preparation of fab-nondestructive antibody-drug conjugates with ultrahigh drug-to-antibody ratio, *Adv. Mater.*, 2023, **35**, 2300377.
18 X. Wang, G. Liu, N. Chen, J. Wu, J. Zhang, Y. Qian, L. Zhang, D. Zhou and Y. Yu, Angiopep2-conjugated star-shaped polyprodrug amphiphiles for simultaneous glioma-targeting therapy and MR imaging, *ACS Appl. Mater. Interfaces*, 2020, **12**, 12143–12154.
19 D. Wang, N. Zhang, T. Yang, X. Jing and L. Meng, Construction polyprodrugs by click-reactions and metal-coordination: pH-responsive release for magnetic resonance imaging guided chemotherapy, *Chem. Eng. J.*, 2021, **422**, 130108.
20 R. García-Vázquez, U. M. Battisti, V. Shalgunov, G. Schäfer, M. Barz and M. M. Herth, [^{11}C]Carboxylated tetrazines for facile labeling of trans-cyclooctene-functionalized Pepto-Brushes, *Macromol. Rapid Commun.*, 2022, **43**, 2100655.
21 M. Müllner, Molecular polymer bottlebrushes in nanomedicine: therapeutic and diagnostic applications, *Chem. Commun.*, 2022, **58**, 5683–5716.
22 G. Feng and B. Liu, Multifunctional AIEgens for future theranostics, *Small*, 2016, **12**, 6528–6535.
23 X. Hu, Z. Chen, H. Ao, Q. Fan, Z. Yang and W. Huang, Rational molecular engineering of organic semiconducting nanoplatforms for advancing NIR-II fluorescence theranostics, *Adv. Opt. Mater.*, 2022, **10**, 2201067.
24 L. Zhang, Y. Liu, H. Huang, H. Xie, B. Zhang, W. Xia and B. Guo, Multifunctional nanotheranostics for near infrared optical imaging-guided treatment of brain tumors, *Adv. Drug Delivery Rev.*, 2022, **190**, 114536.
25 Q. Wei, D. Xu, T. Li, X. He, J. Wang, Y. Zhao and L. Chen, Recent advances of NIR-II emissive semiconducting polymer dots for in vivo tumor fluorescence imaging and theranostics, *Biosensors*, 2022, **12**, 1126.
26 X. Zhao, H. Lei, Y. Cheng, Y. Wu, M. Zhang, G. He, D. Pei, Z. Dong, A. Li and Y. Zhang, A polymeric prodrug for non-invasive, real-time reporting drug release based on ''turn-on'' fluorescent probes, *React. Funct. Polym.*, 2020, **154**, 104649.

27 B. Liu, R. Wu, S. Gong, H. Xiao and S. Thayumanavan, In situ formation of polymeric nanoassemblies using an efficient reversible click reaction, *Angew. Chem., Int. Ed.*, 2020, **59**, 15135–15140.
28 N. Zhang, D. Wang, X. Jing, T. Yang, H. Yang and L. Meng, pH/ROS dual-responsive polymer–drug-based nanocarriers: click-reaction preparation and fluorescence imaging-guided chemotherapy and photodynamic therapy, *ACS Appl. Bio Mater.*, 2021, **4**, 6294–6303.
29 A. Creamer, A. Fiego, A. Agliano, L. Prados-Martin, H. Høgset, A. Najer, D. A. Richards, J. P. Wojciechowski, J. E. J. Foote, N. Kim, A. Monahan, J. Tang, A. Shamsabadi, L. N. C. Rochet, I. A. Thanasi, L. R. de la Ballina, C. L. Rapley, S. Turnock, E. A. Love, L. Bugeon, M. J. Dallman, M. Heeney, G. Kramer-Marek, V. Chudasama, F. Fenaroli and M. M. Stevens, Modular synthesis of semiconducting graft copolymers to achieve ''clickable'' fluorescent nanoparticles with long circulation and specific cancer targeting, *Adv. Mater.*, 2024, **36**, 2300413.
30 M. Gon, K. Tanaka and Y. Chujo, Discovery of functional luminescence properties based on flexible and bendable boron-fused azomethine/azobenzene complexes with O,N,O-type tridentate ligands, *Chem. Rec.*, 2021, **21**, 1358–1373.
31 M. Gon, S. Ito, K. Tanaka and Y. Chujo, Design strategies and recent results for near-infrared-emissive materials based on element-block π-conjugated polymers, *Bull. Chem. Soc. Jpn.*, 2021, **94**, 2290–2301.
32 M. Gon, K. Tanaka and Y. Chujo, A highly efficient near-infrared-emissive copolymer with a N═N double-bond π-conjugated system based on a fused azobenzene–boron complex, *Angew. Chem., Int. Ed.*, 2018, **57**, 6546–6551.
33 M. Gon, J. Wakabayashi, M. Nakamura, K. Tanaka and Y. Chujo, Controlling energy gaps of π-conjugated polymers by multi-fluorinated boron-fused azobenzene acceptors for highly efficient near-infrared emission, *Chem. – Asian J.*, 2021, **16**, 696–703.
34 M. Nakamura, I. Kanetani, M. Gon and K. Tanaka, NIR-II absorption/fluorescence of D–A π-conjugated polymers composed of strong electron acceptors based on boron-fused azobenzene complexes, *Angew. Chem., Int. Ed.*, 2024, **63**, e202404178.
35 M. Gon, J. Wakabayashi, M. Nakamura, K. Tanaka and Y. Chujo, Preparation of near-infrared emissive π-conjugated polymer films based on boron-fused azobenzene complexes with perpendicularly protruded aryl substituents, *Macromol. Rapid Commun.*, 2021, **42**, 2000566.
36 M. Nakamura, M. Gon, K. Tanaka and Y. Chujo, Solid-state near-infrared emission of π-conjugated polymers consisting of boron complexes with vertically projected steric substituents, *Macromolecules*, 2023, **56**, 2709–2718.
37 M. Nakamura, M. Yamauchi, M. Gon and K. Tanaka, UV-to-NIR wavelength conversion of π-conjugated polymers based on pyrene-substituted boron-fused azobenzene complexes, *Macromolecules*, 2023, **56**, 7571–7578.
38 M. Miyata and Y. Chujo, π-Conjugated organoboron polymer as an anion sensor, *Polym. J.*, 2002, **34**, 967–969.
39 L. Ji, S. Griesbeck and T. B. Marder, Recent developments in and perspectives on three-coordinate boron materials: a bright future, *Chem. Sci.*, 2017, **8**, 846–863.
40 H. Li and F. Jäkle, Universal scaffold for fluorescent conjugated organoborane polymers, *Angew. Chem., Int. Ed.*, 2009, **48**, 2313–2316.
41 Y. Adachi, F. Arai, M. Sakabe and J. Ohshita, Effect of the conjugation pathway on the electronic structures of p–π* conjugated polymers with fused borepin units, *Polym. Chem.*, 2021, **12**, 3471–3477.
42 I. A. Adams and P. A. Rupar, A poly(9-borafluorene) homopolymer: an electron-deficient polyfluorene with ''turn-on'' fluorescence sensing of NH_3 vapor, *Macromol. Rapid Commun.*, 2015, **36**, 1336–1340.
43 Y. Shi, J. Li, Z. Zhang, D. Duan, Z. Zhang, H. Liu, T. Liu and Z. Liu, Tracing boron with fluorescence and positron emission tomography imaging of boronated porphyrin nanocomplex for imaging-guided boron neutron capture therapy, *ACS Appl. Mater. Interfaces*, 2018, **10**, 43387–43395.
44 P. Labra-Vázquez, R. Flores-Cruz, A. Galindo-Hernández, J. Cabrera-González, C. Guzmán-Cedillo, A. Jiménez-Sánchez, P. G. Lacroix, R. Santillan, N. Farfán and R. Núñez, Tuning the cell uptake and subcellular distribution in BODIPY–carboranyl dyads: an experimental and theoretical study, *Chem. – Eur. J.*, 2020, **26**, 16530–16540.
45 S. O. Oloo, K. M. Smith and M. D. G. H. Vicente, Multifunctional boron-delivery agents for boron neutron capture therapy of cancers, *Cancers*, 2023, **15**, 3277.
46 A. Van Belois, R. R. Maar, M. S. Workentin and J. B. Gilroy, Dialkynylborane complexes of formazanate ligands: synthesis, electronic properties, and reactivity, *Inorg. Chem.*, 2019, **58**, 834–843.
47 B. Zu, Y. Guo and C. He, Catalytic enantioselective construction of chiroptical boron-stereogenic compounds, *J. Am. Chem. Soc.*, 2021, **143**, 16302–16310.
48 R. Yoshii, K. Tanaka and Y. Chujo, Conjugated polymers based on tautomeric units: regulation of main-chain conjugation and expression of aggregation induced emission property via boron-complexation, *Macromolecules*, 2014, **47**, 2268–2278.
49 X. Guo, Q. Liao, E. F. Manley, Z. Wu, Y. Wang, W. Wang, T. Yang, Y.-E. Shin, X. Cheng, Y. Liang, L. X. Chen, K.-J. Baeg, T. J. Marks and X. Guo, Materials design via optimized intramolecular noncovalent interactions for high-performance organic semiconductors, *Chem. Mater.*, 2016, **28**, 2449–2460.
50 A. B. Pangborn, M. A. Giardello, R. H. Grubbs, R. K. Rosen and F. J. Timmers, Safe and convenient procedure for solvent purification, *Organometallics*, 1996, **15**, 1518–1520.

